The Design Of Repeatable Controls For Kinematically Redundant Robots

Rodney G. Roberts Anthony A. Maciejewski

School of Electrical Engineering
Purdue University
West Lafayette, Indiana 47907

Abstract—**Kinematically redundant manipulators, by definition, possess an infinite number of generalized inverse control strategies for solving the Jacobian equation. These control strategies are not, in general, repeatable in the sense that closed trajectories for the end effector do not result in closed trajectories in the joint space. Two methods for generating control strategies which are repeatable are presented in this work. The first method, which requires one to solve a set of partial differential equations, may be difficult to apply to complicated manipulators thus motivating the second method, which assumes a certain form for the control strategies. Both of these methods result in a technique for designing a repeatable control which is nearest, in an integral norm sense, to a desired optimal control. The desired optimal control is allowed to take the form of any generalized inverse. An example is presented for both methods which illustrates the capability of designing repeatable controls that approximate the behavior of desired optimal inverses in selected regions of the workspace. Finally a comparison of the two methods is made by studying the results of an example simulation.**

I. INTRODUCTION

Kinematically redundant manipulators are robotic systems which possess more degrees of freedom than are required to perform a specified task. For single arm manipulators the task is usually specified as a location or path for the end effector. A manipulator can be described by its kinematic equation

$$\mathbf{x} = \mathbf{f}(\theta) \tag{1}$$

where $\mathbf{x} \in I\!R^m$ represents the workspace position and/or orientation of the end effector and $\theta \in I\!R^n$ represents the manipulator's joint configuration. Thus $m < n$ by definition for redundant manipulators. The Jacobian equation relates the joint velocities to the end effector velocities and is obtained by differentiating (1), resulting in

$$\dot{\mathbf{x}} = J\dot{\theta}. \tag{2}$$

Manuscript received May 20, 1991. This work was supported in part by grants from NEC and TRW.

Due to the extra degrees of freedom, redundant manipulators possess an infinite number of local control schemes of the form

$$\dot{\theta} = G\dot{\mathbf{x}} \tag{3}$$

where $JG = I$ (except at singularities of J or possibly G) in order to satisfy the constraint of a given end effector velocity. A popular local control scheme is pseudoinverse control due to its desirable minimum norm property.

A generalized inverse control like the one given in (3) may not be repeatable in the sense that closed trajectories in the workspace may not be mapped to closed trajectories in the joint space. Pseudoinverse control is no exception as Klein and Huang [2] have shown. When a cyclic task is performed using a nonrepeatable control, the joint angles of the manipulator do not necessarily return to their initial position. In other words, generalized inverse control of kinematically redundant manipulators may produce a drift in joint space when a cyclic task is performed in the workspace. This may pose a problem since the manipulator's behavior would be hard to predict without prior analysis. By using a repeatable control the setup time for a manipulator can be reduced for cyclic tasks since one would only need to check one cycle to see if the manipulator functioned as desired.

Shamir and Yomdin [4] have developed an elegant test using Frobenius's theorem from differential geometry for determining whether or not an arbitrary inverse is repeatable in an open subset of the joint space. This test, called the Lie Bracket Condition (LBC), is formulated in terms of the Lie bracket of the columns of the inverse. The Lie bracket of two vectors $\mathbf{u}$ and $\mathbf{v}$, where both vectors are functions of θ, is given by

$$[\mathbf{u}, \mathbf{v}] = \left(\frac{\partial \mathbf{v}}{\partial \theta}\right)\mathbf{u} - \left(\frac{\partial \mathbf{u}}{\partial \theta}\right)\mathbf{v}. \tag{4}$$

An inverse G is said to satisfy the LBC if the Lie bracket of any two columns of G is in the column space of G. For the special case of the pseudoinverse one need only apply the LBC to J^T which greatly simplifies the computations required.

The remainder of this paper is organized in the following manner: Section II presents two methods for generating repeatable solutions. After a class of repeatable

solutions is found, a technique for determining the member of this class which is nearest to a desired inverse in an integral norm sense is discussed. Section III then illustrates these two design techniques with a specific example. Simulation results are then presented in Section IV with conclusions appearing in Section V.

II. A CLASS OF REPEATABLE INVERSES

This section illustrates two methods for generating a class of repeatable solutions. These inverses, like the extended Jacobian [1], have foliations of stable surfaces and so are guaranteed to be repeatable. The inverses under consideration are generalized inverses like those described by (3). For a manipulator with a single degree of redundancy, any of these inverses can be written in the form

$$G = J^+ + \hat{\mathbf{n}}_J \mathbf{w}^T \tag{5}$$

where $\hat{\mathbf{n}}_J$ is the unit length null vector of the Jacobian J and $\mathbf{w}$ is a vector which uniquely determines G. This follows from the fact that $J(G - J^+) = [0]$. From (5) it is easy to verify that

$$\mathbf{n}_G = J^T \mathbf{w} - \hat{\mathbf{n}}_J. \tag{6}$$

is a null vector of G^T.

In order to implement the first method for designing an optimal repeatable inverse it is necessary to determine a class of vector functions $\mathbf{w}$ which characterize a set of repeatable inverses. This can be done by determining a set of the $\mathbf{w}$ that satisfy the differential equations given by

$$\mathbf{n}_G^T[\mathbf{g}_i, \mathbf{g}_j] = 0 \qquad 1 \le i < j \le m. \tag{7}$$

For three-link planar manipulators (7) simplifies to

$$\mathbf{n}_G \cdot \nabla \times \mathbf{n}_G = 0. \tag{8}$$

Equation (7), or (8) where applicable, determines a class of admissible $\mathbf{w}$ so that for any $\mathbf{w}$ in this class the corresponding inverse G_r is repeatable.

There are infinitely many such repeatable inverses so that it is possible to optimize over this class in order to obtain additional desirable properties. One possible approach is to minimize the distance to an unrepeatable inverse G_d that possesses some desirable characteristics. The measure that will be used in this work is

$$\int_\Omega \|G_r - G_d\|_2^2 \, d\theta \tag{9}$$

where $\|\cdot\|_2$ is the Euclidean norm. Equation (9) gives a measure of the closeness of the two inverses over the connected subset Ω of the joint space. From (5) it follows that

$$\begin{aligned} \|G_r - G_d\|_2 &= \|(J^+ + \hat{\mathbf{n}}_J \mathbf{w}_r^T) - (J^+ + \hat{\mathbf{n}}_J \mathbf{w}_d^T)\|_2 \\ &= \|\hat{\mathbf{n}}_J (\mathbf{w}_r - \mathbf{w}_d)^T\|_2 \end{aligned} \tag{10}$$

where $\mathbf{w}_d$ is the unique vector that corresponds to G_d. Since $\hat{\mathbf{n}}_J$ is of unit length, (9) becomes

$$\int_\Omega \|G_r - G_d\|_2^2 \, d\theta = \int_\Omega \|\mathbf{w}_r - \mathbf{w}_d\|_2^2 \, d\theta \tag{11}$$

which greatly simplifies the computations.

Unfortunately solving for closed form analytical solutions to a set of partial differential equations such as (7) may be a difficult if not impossible task. In order to find a near optimal repeatable control for more complicated manipulators it is necessary to develop a second method, which does not rely on solving complicated PDE's. This method, which will be called the direct method, uses the known geometrical properties of repeatable inverses to generate a subset of analytic solutions to these PDE's by utilizing gradient functions. While this technique has the advantage of avoiding complicated PDE's, it's disadvantage is that it optimizes over a smaller subset of repeatable inverses.

In order to apply this technique a different characterization of the repeatable control strategies, which does not utilize the Lie bracket, is necessary. This method relies on characterizing those vectors which are at every joint value orthogonal to the joint trajectories determined by the control strategy. These vectors are given by the null space of the transpose of the generalized inverse, which for a repeatable generalized inverse is determined by a gradient function. Thus the repeatable strategies can be obtained by inverting the square matrix

$$J_{\mathbf{v}} = \begin{bmatrix} J \\ \mathbf{v}^T \end{bmatrix} \tag{12}$$

where $\mathbf{v}$ is a gradient function which characterizes the repeatable generalized inverse. Note that $J_{\mathbf{v}}$ is of the same form as the extended Jacobian; however, the gradient function may not be related to any physically meaningful function of the joint positions. These repeatable inverses are calculated at nonsingular configurations by taking the first m columns of

$$J_{\mathbf{v}}^{-1} = \begin{bmatrix} G_d - \hat{\mathbf{n}}_J \frac{\mathbf{v}^T G_d}{\hat{\mathbf{n}}_J \cdot \mathbf{v}} & \frac{\hat{\mathbf{n}}_J}{\hat{\mathbf{n}}_J \cdot \mathbf{v}} \end{bmatrix} \tag{13}$$

where once again G_d is some desired (but typically not repeatable) generalized inverse. Thus any repeatable strategy has the form

$$G_r = G_d - \hat{\mathbf{n}}_J \frac{\mathbf{v}^T G_d}{\hat{\mathbf{n}}_J \cdot \mathbf{v}} \tag{14}$$

where $\mathbf{v}$ is a gradient function. From equation (14) it follows that $\mathbf{w}$ is given by

$$\mathbf{w} = -\frac{G_d^T \mathbf{v}}{\hat{\mathbf{n}}_J \cdot \mathbf{v}}. \tag{15}$$

The values of θ which result in $\hat{\mathbf{n}}_J(\theta) \cdot \mathbf{v}(\theta) = 0$, but correspond to nonsingular configurations of the Jacobian, are called algorithmic singularities. These singularities, which were first noted by Baillieul [1] in the case of the extended Jacobian, cause $\|\mathbf{w}\|_2$ to take on infinite values. The cost function, corresponding to (9), on a simply-connected singularity-free subset Ω of the joint space is thus given by

$$\|\mathbf{w}\|_\Omega^2 = \|G_r - G_d\|_\Omega^2 = \int_\Omega \frac{\|G_d^T \mathbf{v}\|_2^2}{(\hat{\mathbf{n}}_J \cdot \mathbf{v})^2}\, d\theta. \tag{16}$$

Since every repeatable control strategy can be written in the form of (14) it is possible to optimize over a set of these strategies by considering a linear space of gradients. Such a space can be given by the span of N linearly independent gradient functions $\{\mathbf{v}_1, \mathbf{v}_2, \ldots, \mathbf{v}_N\}$ so that the augmenting vectors take on the form $\mathbf{v} = \sum_{i=1}^N a_i \mathbf{v}_i$. One must, however, be careful to select these gradient functions in such a way that they are not linear combinations of the rows of J since such a choice would result in a singular augmented Jacobian. One final consideration relates to the fact that all multiples of the gradient function will result in the same control so that a normalization is in order. Such a normalization can be done for example by requiring that $\sum_{i=1}^N a_i^2 = 1$ or by setting some particular a_i equal to one. In some instances it may be possible to make further constraints on the coefficients a_i so that the resulting control strategy contains no algorithmic singularities.

III. AN EXAMPLE

In order to illustrate the two methods described in the previous section, a specific example will be presented. Consider the planar manipulator shown in Fig. 1 which consists of two orthogonal prismatic joints and a third revolute joint of 1 m length. The kinematic function for this manipulator is given by

$$\mathbf{x} = \mathbf{f}(\theta) = \begin{bmatrix} d_1 + \cos\theta_3 \\ d_2 + \sin\theta_3 \end{bmatrix} \tag{17}$$

where $\mathbf{x} = [\,x \quad y\,]^T$ and $\theta = [\,d_1 \quad d_2 \quad \theta_3\,]^T$. It is easy to see that the Jacobian for this manipulator is

$$J = \begin{bmatrix} 1 & 0 & -\sin\theta_3 \\ 0 & 1 & \cos\theta_3 \end{bmatrix}. \tag{18}$$

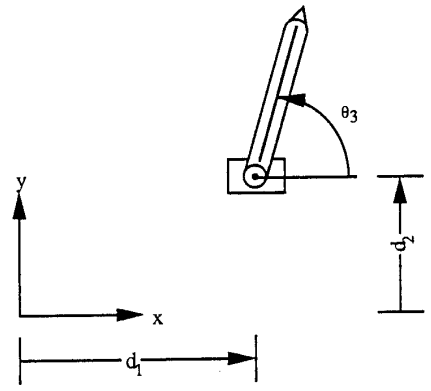

Fig. 1. Geometry of a planar three-link manipulator whose first two joints are prismatic and whose last joint is revolute and of 1 m length.

The first step in determining the repeatable inverse which is closest to the pseudoinverse is to characterize all generalized inverses by their null vectors. By using (6) these vectors can be written as

$$\mathbf{n}_G = \begin{bmatrix} w_1 - \frac{1}{\sqrt{2}}\sin\theta_3 \\ w_2 + \frac{1}{\sqrt{2}}\cos\theta_3 \\ -w_1\sin\theta_3 + w_2\cos\theta_3 - \frac{1}{\sqrt{2}} \end{bmatrix} \tag{19}$$

where they are now parameterized by w_1 and w_2. Next, these null vectors are restricted to those null vectors which correspond to a subset of repeatable inverses. This can be done by determining solutions to the differential equations obtained from (8) and (19). For this particular example the solution of these equations is characterized by the relation

$$w_1 = k w_2 + \frac{1}{\sqrt{2}}(\sin\theta_3 + k\cos\theta_3) \tag{20}$$

where k is an arbitrary constant and it is assumed that the inverses are only functions of θ_3. Thus, (20) parametrizes these repeatable inverses in terms of the function w_2 and the constant k.

Now that a class of repeatable inverses has been derived, the optimal member of this class with respect to an appropriately chosen criterion function can be found. For this example the criterion function is given by

$$C(k) = \int_a^b \|G_r - J^+\|_2^2\, d\theta_3 \tag{21}$$

which is a measure of the distance from the repeatable inverse G_r to the pseudoinverse in the region $a \le \theta_3 \le b$.

It has been shown [3] that the optimal solution must take the form

$$w_1 = \frac{k\cos\theta_3 + \sin\theta_3}{\sqrt{2}(k^2+1)} \tag{22}$$

$$w_2 = -\frac{k(\sin\theta_3 + k\cos\theta_3)}{\sqrt{2}(k^2+1)}. \tag{23}$$

Equations (22) and (23) give a family of repeatable inverses, parameterized by k, that minimize (24). Substituting (22) and (23) into (24) gives

$$\|\mathbf{w}\|_2^2 = \frac{(\sin\theta_3 + k\cos\theta_3)^2}{2(k^2+1)} \tag{24}$$

which is bounded by 1/2 thus insuring that the criterion function is well-defined. Therefore (21) becomes

$$C(k) = \int_a^b \frac{(\sin\theta_3 + k\cos\theta_3)^2}{2(k^2+1)}\, d\theta_3. \tag{25}$$

Note that the optimization resulting in (22) and (23) is independent of a and b, the limits of integration for (25).

The criterion function $C(k)$ can be rewritten as

$$C(k) = \int_a^b \frac{1}{2}\sin^2(\theta_3 + \phi)\, d\theta_3 \tag{26}$$

where $\phi = \tan^{-1} k \in [-\pi/2, \pi/2]$. The cost function $C(k)$ has now been written as a differentiable function of ϕ on the interval $[-\pi/2, \pi/2]$. It then follows that C has a minimum value on this closed interval and that this minimum occurs either at a point where the first derivative of C with respect to ϕ is zero or at an endpoint of the interval. Setting $dC/d\phi$ to zero and applying the second derivative test results in the following optimal solution

$$\phi^* = \begin{cases} -\frac{1}{2}(a+b) + n\pi, & \text{if } 0 < b-a < \pi \\ -\frac{1}{2}(a+b) + \frac{2n+1}{2}\pi, & \text{if } \pi < b-a < 2\pi \end{cases} \tag{27}$$

where n is chosen so that $\phi^* \in [-\pi/2, \pi/2]$. Since ϕ in equation (26) can vary over $\mathbb{R}$ one does not need to check the endpoints $-\pi/2$ and $\pi/2$. Also since (26) is periodic with respect to ϕ with period π, one knows that (27) determines a global minimum. The corresponding k^* is found by taking the tangent of ϕ^* resulting in

$$k^* = \begin{cases} -\tan(\frac{a+b}{2}), & \text{if } 0 < b-a < \pi \\ \cot(\frac{a+b}{2}), & \text{if } \pi < b-a < 2\pi. \end{cases} \tag{28}$$

Note that infinite values of k^* are allowable and that this in fact does correspond to an inverse which is given by the limit of equations (22) and (23) as k approaches $\pm\infty$. Thus for $k = \pm\infty$ the inverse is given by taking $w_1 = 0$ and $w_2 = -\frac{1}{\sqrt{2}}\cos\theta_3$.

The second method described in the previous section, which consists of augmenting the Jacobian with a gradient function, can also be used. Consider augmenting vectors of the form $\mathbf{v} = \alpha\mathbf{e}_1 + \beta\mathbf{e}_2 + \gamma\mathbf{e}_3$ where $\mathbf{e}_1$, $\mathbf{e}_2$, and $\mathbf{e}_3$ represent the standard basis for $\mathbb{R}^3$. Clearly any such vector function is a gradient, and since it is not a function of d_1 or d_2, the resulting repeatable control strategy will be a function of θ_3 only. Therefore, in this case the resulting optimal solution for the direct method cannot be better than the one obtained above, which optimizes over all repeatable control strategies which are functions of θ_3 only. Thus the solution resulting from the direct method can be considered an approximation of the optimal solution obtained previously. From (15) it follows that the vector $\mathbf{w}$ is given by

$$\mathbf{w} = \frac{1}{\delta}\begin{bmatrix} \alpha(1+\cos^2\theta_3) + \beta\sin\theta_3\cos\theta_3 - \gamma\sin\theta_3 \\ \alpha\sin\theta_3\cos\theta_3 + \beta(1+\sin^2\theta_3) + \gamma\cos\theta_3 \end{bmatrix} \tag{29}$$

where $\delta = \sqrt{2}(\alpha\sin\theta_3 - \beta\cos\theta_3 + \gamma)$. Under the simple coordinate transformation $r = \sqrt{\alpha^2+\beta^2}$ and $\psi = \arctan(-\alpha/\beta)$ it follows that

$$\|\mathbf{w}\|_2^2 = \frac{2r^2}{\Delta^2} + \frac{2\gamma}{\Delta} - \frac{3}{2} \tag{30}$$

where $\Delta = \gamma + r\cos(\theta_3 - \psi)$. Algorithmic singularities for this control strategy will occur when $\Delta = 0$. This problem can be remedied by either requiring $\gamma + r\cos(\theta_3 - \psi)$ to be strictly positive or strictly negative. Such a restriction would require γ to be nonzero, and since any multiple of $\mathbf{v}$ results in the same control, γ can be, without loss of generality, taken to be 1. Thus in order to eliminate algorithmic singularities one requires that $1 + r\cos(\theta_3 - \psi) > 0$, or equivalently that $0 \le r < 1$. In this example the values or r will be restricted to lie in the closed interval $[0, 0.9]$.

As before the cost function has the form

$$C(r,\psi) = \int_a^b \|\mathbf{w}\|_2^2\, d\theta_3 \tag{31}$$

where now the dependence is on the variables r and ψ. Substituting (30) into (31) yields

$$C(r,\psi) = 2\int_a^b \left(\frac{r^2}{\Delta^2} + \frac{1}{\Delta}\right) d\theta_3 - \frac{3(b-a)}{2} \tag{32}$$

where $\gamma = 1$. Applications of the first and second derivative test individually to the first two terms of (32) shows that the optimal ψ is given by

$$\psi^* = \frac{1}{2}(a+b) \tag{33}$$

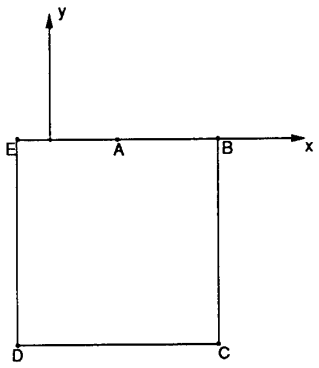

Fig. 2. The desired end effector trajectory (3 m square) used in the simulation of the manipulator depicted in Fig. 1.

for intervals of less than 2π. For θ_3 intervals $[a, b]$ of length less than $\pi/6$ the optimal r is given by 0.9. This follows readily from the fact that the first derivative of $\|\mathbf{w}\|_2$ with respect to r is strictly negative for $|\theta_3| \leq \pi/12$ and $0 \leq r \leq 0.9$. Thus the optimal coefficients are $\alpha = 0$, $\beta = -0.9$, and $\gamma = 1$. The resulting $\mathbf{w}$ is

$$\mathbf{w} = \frac{1}{\sqrt{2}} \begin{bmatrix} \sin\theta_3 \\ -\cos\theta_3 + \frac{1.8}{1+0.9\cos\theta_3} \end{bmatrix}. \qquad (34)$$

IV. SIMULATION

In order to compare the two methods used in the example in Section III, this section presents simulation results for the manipulator depicted in Fig. 1, commanded to follow the 3 m square end effector trajectory shown in Fig. 2. The manipulator's initial configuration is set to the origin of the joint space which corresponds to the point $(x, y) = (1, 0)$ in the workspace. The joint space trajectory obtained using pseudoinverse control is shown in Fig. 3. As expected, pseudoinverse control produces a drift in the joint space which results in a joint trajectory which spirals down the fiber corresponding to the point $(1, 0)$ in the workspace. Superimposed on this figure are the two stable surfaces which correspond to the optimal repeatable inverse, which was designed to approximate the pseudoinverse in the θ_3 region $[-\pi/12, \pi/12]$, and the approximation to this optimal obtained by applying the direct method. Clearly, the pseudoinverse trajectory initially lies on both of these stable surfaces, as designed, but starts to diverge as the end effector leaves point C. It is at this point that the global repeatability requirement forces the repeatable inverse to abandon the desired pseudoinverse solution.

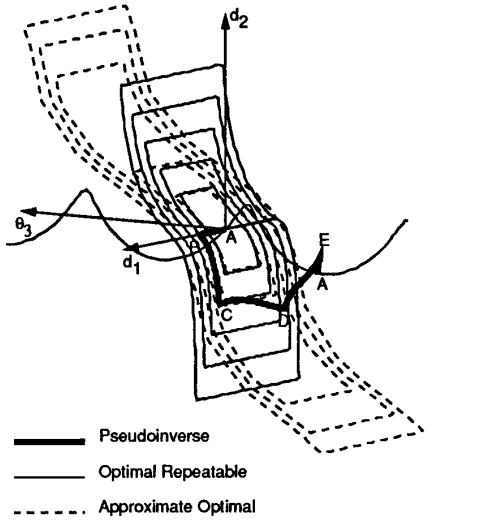

Fig. 3. A 3D view of the joint space trajectory corresponding to pseudoinverse control for the manipulator in Fig. 1. The stable surfaces for the optimal repeatable control and the approximate optimal repeatable control are also shown.

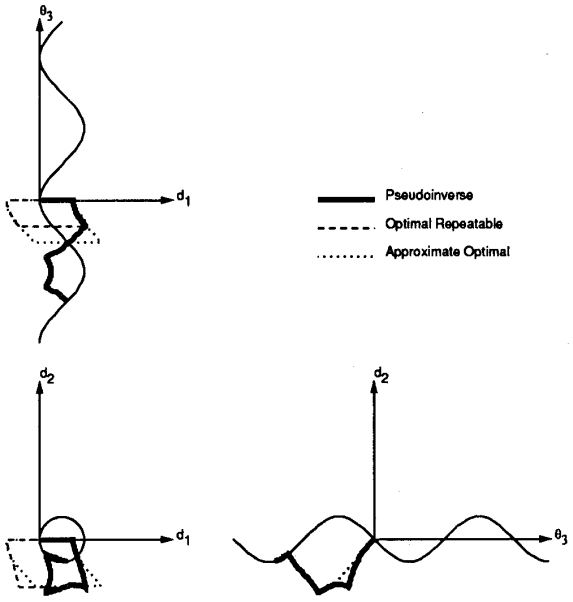

Fig. 4. Three orthogonal views of the joint space trajectories obtained using pseudoinverse control, the optimal repeatable control, and the approximate optimal repeatable control for the end effector path in Fig. 2.

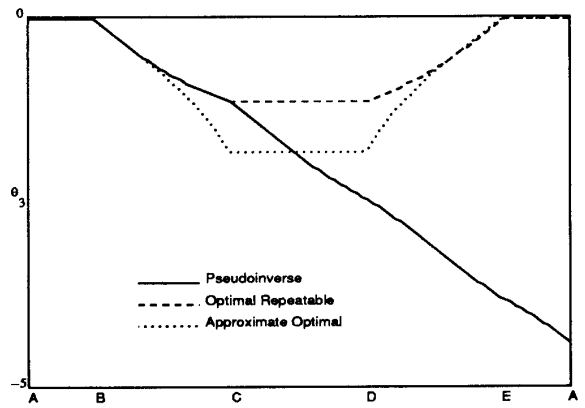

Fig. 5. A plot of θ_3, which together with the end effector position uniquely identifies the configuration of the manipulator shown in Fig. 1, as a function of the position of the end effector in the workspace for the trajectory used in Fig. 2.

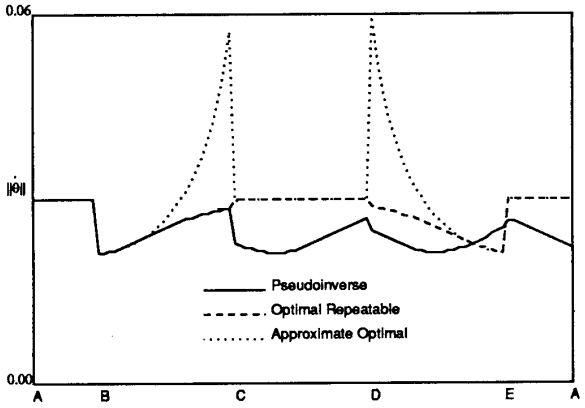

Fig. 6. A plot of the joint velocity norm as a function of the position of the end effector in the workspace for the trajectory used in Fig. 2.

Fig. 4 provides a direct comparison of the resulting joint space trajectories when these three different control techniques are used to follow the desired end effector trajectory specified in Fig. 2. Both of the repeatable controls provide quite good approximations to the pseudoinverse in the design region, i.e. in the neighborhood of A. This is more clearly illustrated in Fig. 5 which in effect plots the configuration of the manipulator, since any joint value uniquely identifies the configuration, along the specified end effector trajectory. It is easy to see from this figure that the optimal repeatable inverse solution exactly matches the performance of the pseudoinverse trajectory up to the point C. The approximation to the optimal repeatable inverse is likewise quite good until about halfway between point B and C. The norm of the joint velocity for these three trajectories is presented in Fig. 6. This figure illustrates the tradeoff resulting from the use of the approximate optimal inverse. Note that outside of the design region, i.e. the limits of integration on (31), the performance of the approximate inverse can be quite poor, as is the case near C and D.

V. CONCLUSIONS

The constraint of repeatability for all end effector trajectories and all initial conditions, which is characterized by foliations of stable surfaces, significantly restricts the choice of available generalized inverse controls. However, it has been shown that it is possible to approximate the behavior of any desirable optimal inverse in a specified region by determining the repeatable inverse that is closest to the desired inverse. This results in a controlwhich takes advantage of the available redundancy to locally optimize some desirable performance criterion in the specified region of the workspace while also satisfying the extremely restrictive global constraint of repeatability.

REFERENCES

[1] J. Baillieul, "Kinematic programming alternatives for redundant manipulators," in *Proc. 1985 IEEE Int. Conf. Robotics Automat.* (St. Louis, MO, March 25-28, 1985), pp. 722-728.

[2] C.A. Klein and C.H. Huang, "Review of pseudoinverse control for use with kinematically redundant manipulators," *IEEE Trans. on Syst., Man Cyber.*, vol. SMC-13, no. 3, pp. 245-250, March/April 1983.

[3] R.G. Roberts and A.A. Maciejewski, "Near pseudoinverse control of kinematically redundant manipulators with the constraint of repeatability," in *Proc. 1991 IEEE Int. Conf. Syst. Eng.* (Dayton, OH, August 1-3, 1991).

[4] T. Shamir and Y. Yomdin, "Repeatability of redundant manipulators: mathematical solution of the problem," *IEEE Trans. Automatic Control*, vol. 33, no. 11, pp. 1004-1009, Nov. 1988.